

## Synthesis and Biological Evaluation of Low Molecular Weight Fluorescent Imaging Agents for the Prostate-Specific Membrane Antigen

Ying Chen, Mrudula Pullambhatla, Sangeeta Ray Banerjee, Youngjoo Byun, Marigo Stathis, Camilo Rojas, Barbara S. Slusher, Ronnie C Mease, and Martin G Pomper

*Bioconjugate Chem.*, **Just Accepted Manuscript** • DOI: 10.1021/bc3003919 • Publication Date (Web): 19 Nov 2012

Downloaded from <http://pubs.acs.org> on November 27, 2012

### Just Accepted

"Just Accepted" manuscripts have been peer-reviewed and accepted for publication. They are posted online prior to technical editing, formatting for publication and author proofing. The American Chemical Society provides "Just Accepted" as a free service to the research community to expedite the dissemination of scientific material as soon as possible after acceptance. "Just Accepted" manuscripts appear in full in PDF format accompanied by an HTML abstract. "Just Accepted" manuscripts have been fully peer reviewed, but should not be considered the official version of record. They are accessible to all readers and citable by the Digital Object Identifier (DOI®). "Just Accepted" is an optional service offered to authors. Therefore, the "Just Accepted" Web site may not include all articles that will be published in the journal. After a manuscript is technically edited and formatted, it will be removed from the "Just Accepted" Web site and published as an ASAP article. Note that technical editing may introduce minor changes to the manuscript text and/or graphics which could affect content, and all legal disclaimers and ethical guidelines that apply to the journal pertain. ACS cannot be held responsible for errors or consequences arising from the use of information contained in these "Just Accepted" manuscripts.



**ACS Publications**  
High quality. High impact.

Bioconjugate Chemistry is published by the American Chemical Society, 1155 Sixteenth Street N.W., Washington, DC 20036  
Published by American Chemical Society. Copyright © American Chemical Society. However, no copyright claim is made to original U.S. Government works, or works produced by employees of any Commonwealth realm Crown government in the course of their duties.

**Synthesis and Biological Evaluation of Low Molecular Weight Fluorescent Imaging  
Agents for the Prostate-Specific Membrane Antigen**

Ying Chen,<sup>1</sup> Mrudula Pullambhatla,<sup>1</sup> Sangeeta R. Banerjee,<sup>1</sup> Youngjoo Byun,<sup>2</sup> Marigo  
Stathis,<sup>3</sup> Camilo Rojas,<sup>3</sup> Barbara S. Slusher,<sup>3</sup> Ronnie C. Mease,<sup>1</sup> Martin G. Pomper<sup>1</sup>

<sup>1</sup>Russell H. Morgan Department of Radiology, Johns Hopkins Medical School,  
Baltimore, MD 21231, USA

<sup>2</sup>College of Pharmacy, Korea University, 2511 Sejong-ro, Jochiwon-eup, Yeongi-gun,  
Chungnam 339-700, South Korea

<sup>3</sup>NeuroTranslational Drug Discovery Program, Brain Science Institute, Johns Hopkins  
Medical School, Baltimore, MD 21231, USA

Corresponding author: Martin G. Pomper, M.D., Ph.D.  
Johns Hopkins Medical School  
1550 Orleans Street, 492 CRB II  
Phone: 410-955-2789  
Fax: 443-817-0990  
Email: [mpomper@jhmi.edu](mailto:mpomper@jhmi.edu)

**ABSTRACT**

Targeted near-infrared (NIR) optical imaging can be used *in vivo* to detect specific tissues, including malignant cells. A series of NIR fluorescent ligands targeting the prostate-specific membrane antigen (PSMA) was synthesized and each tested for its ability to image PSMA+ tissues in experimental models of prostate cancer.

The agents were prepared by conjugating commercially available active esters of NIR dyes, including IRDye800CW, IRDye800RS, Cy5.5, Cy7 or a derivative of indocyanine green (ICG) to the terminal amine group of (*S*)-2-(3-((*S*)-5-amino-1-carboxypentyl)ureido)pentanedioic acid **1**, (14*S*,18*S*)-1-amino-8,16-dioxo-3,6-dioxo-9,15,17-triazaicosane-14,18,20-tricarboxylic acid **2** and (3*S*,7*S*)-26-amino-5,13,20-trioxo-4,6,12,21-tetraazahexacosane-1,3,7,22-tetracarboxylic acid **3**. The  $K_i$  values for the dye-inhibitor conjugates ranged from 1 – 700 pM. All compounds proved capable of imaging PSMA+ tumors selectively to varying degrees depending on the choice of fluorophore and linker. The highest tumor uptake was observed with IRDye800CW employing a polyethylene glycol or lysine-suberate linker, as in 800CW-**2** and 800CW-**3**, while the highest tumor to non-target tissue ratios were obtained for Cy7 with these same linkers, as in Cy7-**2** and Cy7-**3**. Compounds **2** and **3** provide useful scaffolds for targeting of PSMA+ tissues *in vivo* and should be useful for preparing NIR dye conjugates designed specifically for clinical intra-operative optical imaging devices.

## INTRODUCTION

The National Cancer Institute estimates 241,740 new cases and 28,170 new deaths from prostate cancer (PCa) in 2012.<sup>1</sup> PCa is the second leading cause of cancer-related death in men. Surgery is the most commonly used treatment for clinically localized PCa and provides a survival advantage compared to watchful waiting.<sup>2</sup> A pressing issue in surgery for PCa is the assurance of a complete resection of the tumor, namely, a negative surgical margin. A positive surgical margin necessitates adjuvant radiation therapy, which is required in up to 27.8% of patients<sup>3</sup> compared to 9.1% of men undergoing radical retropubic prostatectomy. Given that currently more than 50,000 radical prostatectomies are performed annually, these statistics would suggest that more than 9,000 men are undergoing unnecessary adjuvant radiation therapy.<sup>4</sup> Given that such radiation therapy costs in excess of \$25,000 per patient, the estimated cost of preventable positive margins is at least \$225M annually.

Local tumor invasion can be difficult to assess pre- and even intra-operatively, but its detection during surgery can be augmented through the use of fluorescent dyes that home to tumor in conjunction with an excitation laser and camera that are tuned to the excitation and emission wavelengths of the dye employed.<sup>5-7</sup> While such intra-operative tumor detection has been performed using non-targeted agents,<sup>8</sup> targeted agents are coming online.<sup>9,10</sup> Because of superior tissue penetration and less interference from the presence of blood in the surgical field, dyes with emission wavelengths in the near-infrared (NIR) region of the spectrum (650 – 900 nm) are generally employed for this purpose.<sup>11</sup> Because of its abundant expression on the surface of PCa<sup>12,13</sup> as well as

1  
2  
3 within most solid tumor neovasculature,<sup>14-17</sup> we have developed a series of NIR-emitting  
4  
5  
6 dyes that target the prostate-specific membrane antigen (PSMA).  
7  
8  
9

10 We and others have synthesized a variety of low molecular weight PSMA-targeting  
11  
12 radiotracers to enable imaging of PCa, with several such agents currently in the clinic.<sup>18-</sup>  
13  
14  
15 <sup>21</sup> Optical agents have also been synthesized,<sup>22-24</sup> and we have previously tested one such  
16  
17 compound *in mice* to good effect.<sup>9</sup> While a variety of radiolabeled PSMA-targeting  
18  
19 antibodies have been used for tumor imaging,<sup>25-27</sup> we prefer agents of low molecular  
20  
21 weight due to more tractable pharmacokinetics, namely, more rapid washout from non-  
22  
23 target sites enabling imaging within hours rather than days of administration.  
24  
25  
26  
27  
28

29 NIR-emitting optical dyes are relatively large organic molecules with extended  
30  
31 conjugation, which presents two potential difficulties for target acquisition *in vivo*: 1)  
32  
33 steric hindrance when linked to small affinity agents, such as the ureas present in many of  
34  
35 the above mentioned PSMA inhibitors; and, 2) poor pharmacokinetics. Recently, we  
36  
37 reported the preparation and evaluation *in vivo* of YC-27 (800CW-**3**), which contains a  
38  
39 lysine-suberate linker between the dye (IRDye800CW, LI-COR Biosciences, Lincoln,  
40  
41 NE) and the PSMA targeting urea.<sup>9</sup> With 800CW-**3** we were able to visualize a PSMA+  
42  
43 tumor xenograft by optical imaging, demonstrating that with a long lysine-suberate  
44  
45 linking moiety, i.e., a long linker, PSMA inhibitors containing bulky groups will still bind  
46  
47 to the target. Here we extend this work by synthesizing and testing a series of PSMA-  
48  
49 targeted NIR fluorescent agents, each containing either no linker, or one of two different  
50  
51 linking groups that have different pharmacokinetic implications for imaging *in vivo*.  
52  
53  
54  
55  
56  
57  
58  
59  
60

## EXPERIMENTAL PROCEDURES

**Chemistry.** *General Methods.* All chemicals and solvents were purchased from either Sigma-Aldrich (Milwaukee, WI) or Fisher Scientific (Pittsburgh, PA). The *N*-hydroxysuccinimide (NHS) esters of IRDye800CW and IRDye800RS were purchased from LI-COR Biosciences. The *N*-hydroxysulfosuccinimide ester of ICG derivative (ICG-sulfo-OSu) was purchased from DOJINDO Molecular Technologies (Rockville, MD). The NHS esters of Cy7 and Cy5.5 were purchased from GE Healthcare (Piscataway, NJ). <sup>1</sup>H NMR spectra were obtained on a Bruker Avance 400 MHz Spectrometer (Billerica, MA). Mass spectra were obtained on a Bruker Esquire 3000 plus system (ESI) or an Applied Biosystems Voyager DE-FTR MALDI-TOF (Foster City, CA). High-performance liquid chromatography (HPLC) purifications were performed on a Waters 625 LC system (Milford, MA) or a Varian Prostar System (Varian Medical Systems, Palo Alto, CA). Optical images were obtained using the Pearl Impulse Imager (LI-COR Biosciences, Lincoln, NE) and a Xenogen IVIS Spectrum (Caliper Life Sciences, Hopkinton, MA). HPLC traces of all of the final compounds are available in the Supplementary Information.

**Synthesis of (*S*)-2-(3-((*S*)-5-amino-1-carboxypentyl)ureido)pentanedioic acid (1).** To a solution of (10*S*,14*S*)-tris(4-methoxybenzyl) 2,2-dimethyl-4,12-dioxo-3-oxa-5,11,13-triazahexadecane-10,14,16-tricarboxylate **4**<sup>28</sup> (0.264 g, 0.033 mmol) a solution of 3% anisole in TFA (1 mL) was added and the mixture was reacted at room temperature for 20 min, then concentrated on a rotary evaporator. The crude material was purified by HPLC

[Econosphere C18, 10  $\mu\text{m}$ , 250 x 10 mm,  $\text{H}_2\text{O}/\text{CH}_3\text{CN}/\text{TFA}$  (92/8/0.1), 4 mL/min] to afford 0.108 g (74%) of **1** (retention time = 4 min).  $^1\text{H}$  NMR (400 MHz,  $\text{D}_2\text{O}$ )  $\delta$  4.17-4.25 (m, 2H), 2.94-2.98 (m, 2H), 2.46-2.50 (m, 2H), 2.11-2.19 (m, 1H), 1.80-1.98 (m, 2H), 1.61-1.73 (m, 3H), 1.40-1.49 (m, 2H).  $^{13}\text{C}$  NMR (400 MHz,  $\text{D}_2\text{O}$ ):  $\delta$  176.9, 176.8, 176.2, 163.0, 162.7, 162.3, 162.0, 158.8, 120.2, 117.3, 114.1, 111.5, 52.7, 52.4, 38.8, 30.0, 29.7, 25.8, 25.7, 21.5. ESI-Mass calcd for  $\text{C}_{12}\text{H}_{22}\text{N}_3\text{O}_7$   $[\text{M}]^+$  320.2, found 320.0.

**Synthesis of 800CW-1.** To a solution of **1** (0.5 mg, 1.15  $\mu\text{mol}$ ) in DMSO (0.1 mL) was added *N,N*-diisopropylethylamine (0.002 mL, 11.5  $\mu\text{mol}$ ), followed by the NHS ester of IRDye800CW (0.3 mg, 0.26  $\mu\text{mol}$ ). After 2 h at room temperature the reaction mixture was purified by HPLC (Econosphere C18, 5  $\mu\text{m}$ , 150 x 4.6 mm; mobile phase, A = 0.1% TFA in  $\text{H}_2\text{O}$ , B = 0.1% TFA in  $\text{CH}_3\text{CN}$ ; gradient, 0 min = 5% B, 5 min = 5% B, 45 min = 100% B; flow rate, 1 mL/min) to afford 0.2 mg (60%) of 800CW-1 (retention time = 15 min). ESI-Mass calcd for  $\text{C}_{58}\text{H}_{74}\text{N}_5\text{O}_{21}\text{S}_4$   $[\text{M}]^+$  1304.4, found 1303.8.

**Synthesis of 800RS-1** To a solution of **1** (0.2 mg, 0.46  $\mu\text{mol}$ ) in DMSO (0.05 mL) was added *N,N*-diisopropylethylamine (0.002 mL, 11.5  $\mu\text{mol}$ ), followed by the NHS ester of IRDye800RS (0.2 mg, 0.21  $\mu\text{mol}$ ). After 2 h at room temperature the reaction mixture was purified by HPLC as described for 800CW-1 to afford 0.2 mg (84%) of 800RS-1 (retention time = 23 min). ESI-Mass calcd for  $\text{C}_{58}\text{H}_{73}\text{N}_5\text{O}_{15}\text{S}_2$   $[\text{M}]^+$  1143.5, found 1143.5.  $[\text{M}+\text{H}]^{2+}$ , 1144.0  $[\text{M}]^+$ .

**Synthesis of ICG-1.** To a solution of **1** (0.2 mg, 0.46  $\mu\text{mol}$ ) in DMSO (0.1 mL) was added *N,N*-diisopropylethylamine (0.002 mL, 11.5  $\mu\text{mol}$ ), followed by ICG-sulfo-OSu (0.3 mg, 0.32  $\mu\text{mol}$ ). After 2 h at room temperature the reaction mixture was purified by HPLC as described for 800CW-**1** to afford 0.2 mg (60%) of ICG-**1** (retention time = 24 min). ESI-Mass calcd for  $\text{C}_{57}\text{H}_{69}\text{N}_5\text{O}_{11}\text{S}$   $[\text{M}]^+$  1031.5, found 516.5  $[\text{M}+\text{H}]^{2+}$ , 1032.0  $[\text{M}]^+$ .

**Synthesis of Cy7-1.** To a solution of **1** (0.5 mg, 1.15  $\mu\text{mol}$ ) in DMSO (0.1 mL) was added *N,N*-diisopropylethylamine (0.002 mL, 11.5  $\mu\text{mol}$ ), followed by the NHS ester of Cy7 (0.3 mg, 0.37  $\mu\text{mol}$ ). After 2 h at room temperature the reaction mixture was purified by HPLC as described for 800CW-**1** to afford 0.2 mg (55%) of Cy7-**1** (retention time = 16 min). ESI-Mass calcd for  $\text{C}_{47}\text{H}_{61}\text{N}_5\text{O}_{14}\text{S}_2$   $[\text{M}]^+$  983.4, found 492.5  $[\text{M}+\text{H}]^{2+}$ , 984.0  $[\text{M}]^+$ .

**Synthesis of Cy5.5-1.** To a solution of **1** (0.5 mg, 1.15  $\mu\text{mol}$ ) in DMSO (0.1 mL) was added *N,N*-diisopropylethylamine (0.002 mL, 11.5  $\mu\text{mol}$ ), followed by the NHS ester of Cy5.5 (0.3 mg, 0.27  $\mu\text{mol}$ ). After 2 h at room temperature the reaction mixture was purified by HPLC as described for 800CW-**1** to afford 0.2 mg (62%) of Cy5.5-**1** (retention time = 14 min). ESI-Mass calcd for  $\text{C}_{53}\text{H}_{63}\text{N}_5\text{O}_{20}\text{S}_4$   $[\text{M}]^+$  1217.3, found 609.4  $[\text{M}+\text{H}]^{2+}$ , 1217.7  $[\text{M}]^+$ .

**Synthesis of (14*S*,18*S*)-1-amino-8,16-dioxo-3,6-dioxa-9,15,17-triazaicosane-14,18,20-tricarboxylic acid (**2**).** To the tosylate salt of (*S*)-5-(3-((*S*)-1,5-bis((4-



methoxybenzyl)oxy)-1,5-dioxopentan-2-yl)ureido)-6-((4-methoxybenzyl)oxy)-6-oxohexan-1-aminium **5**<sup>28,29</sup> (0.103 g, 0.121 mmol) in DMF (2 mL) was added Boc-NH(CH<sub>2</sub>CH<sub>2</sub>O)<sub>2</sub>CH<sub>2</sub>COOH (0.060 g, 0.135 mmol) and TBTU (0.040g, 0.125 mmol), followed by *N,N*-diisopropylethylamine (0.042 mL, 0.241 mmol). After stirring overnight at room temperature the solvent was evaporated on a rotary evaporator. The crude material was purified by silica gel column chromatography using methanol/methylene chloride (5:95) to give 0.101 g of (14*S*,18*S*)-tris(4-methoxybenzyl) 1-amino-8,16-dioxo-3,6-dioxa-9,15,17-triazaicosane-14,18,20-tricarboxylate, **6** in 90% yield. MALDI-TOF Mass calcd for C<sub>47</sub>H<sub>64</sub>N<sub>4</sub>NaO<sub>15</sub> [M+Na]<sup>+</sup> 947.4, found 947.1. Compound **6** was dissolved in a solution of 3% anisole in TFA (1 mL), allowed to react at room temperature for 10 min, and then concentrated. The crude material was purified by HPLC [Econosphere C18, 10 μm, 250 x 10 mm, H<sub>2</sub>O/CH<sub>3</sub>CN/TFA (92/8/0.1), 4 mL/min] to afford 0.035 g (57%) of **2** (retention time = 11 min ). <sup>1</sup>H NMR (400 MHz, D<sub>2</sub>O) δ 4.17-4.21 (m, 1H), 4.10-4.13 (m, 1H), 4.00 (s, 2H), 3.67-3.71 (m, 6H), 3.14-3.20 (m, 4H), 2.43-2.46 (m, 2H), 2.08-2.13 (m, 1H), 1.87-1.93 (m, 1H), 1.76-1.79 (m, 1H), 1.63-1.67 (m, 1H), 1.45-1.50 (m, 2H), 1.33-1.40 (m, 2H). <sup>13</sup>C NMR (400 MHz, D<sub>2</sub>O): δ 176.9, 176.8, 176.0, 171.7, 163.0, 162.7, 162.3, 162.0, 158.8, 117.3, 114.4, 69.8, 69.0, 65.9, 52.8, 52.2, 38.6, 38.1, 30.1, 29.6, 27.3, 25.8, 21.5. ESI-Mass calcd for C<sub>18</sub>H<sub>33</sub>N<sub>4</sub>O<sub>10</sub> [M]<sup>+</sup> 465.2, found 465.2.

**Synthesis of 800CW-2.** To a solution of compound **2** (0.3 mg, 0.52 μmol) in DMSO (0.05 mL) was added *N,N*-diisopropylethylamine (0.002 mL, 11.5 μmol), followed by the NHS ester of IRDye800CW (0.2 mg, 0.17 μmol). After 2 h at room temperature the

reaction mixture was purified by HPLC (Econosphere C18, 5 $\mu$ m, 150  $\times$  4.6 mm mobile phase, A = 50 mM triethylamine acetate buffer (pH 6.0), B = CH<sub>3</sub>CN; gradient, 0 min = 0% B, 5 min = 0% B, 45 min = 100% B; flow rate, 1 mL/min) to afford 0.2 mg (80%) of 800CW-2 (retention time = 22 min). ESI-Mass calcd for C<sub>64</sub>H<sub>84</sub>N<sub>6</sub>O<sub>24</sub>S<sub>4</sub> [M]<sup>+</sup> 1448.4, found 1448.7.

**Synthesis of 800RS-2.** To a solution of **2** (0.3 mg, 0.52  $\mu$ mol) in DMSO (0.05 mL) was added *N,N*-diisopropylethylamine (0.002 mL, 11.4  $\mu$ mol), followed by the NHS ester of IRDye800RS (0.2 mg, 0.21  $\mu$ mol). After 2 h at room temperature the reaction mixture was purified by HPLC as in 800CW-2 to afford 0.2 mg (75%) of 800RS-2 (retention time = 28 min). ESI-Mass calcd for C<sub>64</sub>H<sub>84</sub>N<sub>6</sub>O<sub>18</sub>S<sub>2</sub> [M]<sup>+</sup> 1288.5, found 1288.9.

**Synthesis of ICG-2.** To a solution of **2** (0.5 mg, 0.86  $\mu$ mol) in DMSO (0.1 mL) was added *N,N*-diisopropylethylamine (0.002 mL, 11.5  $\mu$ mol), followed by ICG-sulfo-OSu (0.3 mg, 0.32  $\mu$ mol). After 2 h at room temperature the reaction mixture was purified by HPLC as described for 800CW-1 to afford 0.2 mg (53%) of ICG-2 (retention time = 26 min). ESI-Mass calcd for C<sub>63</sub>H<sub>80</sub>N<sub>6</sub>O<sub>14</sub>S [M]<sup>+</sup> 1176.5, found 589.1 [M+H]<sup>2+</sup>, 1177.1 [M]<sup>+</sup>.

**Synthesis of Cy7-2.** To a solution of **2** (0.5 mg, 0.86  $\mu$ mol) in DMSO (0.1 mL) was added *N,N*-diisopropylethylamine (0.002 mL, 11.5  $\mu$ mol), followed by the NHS ester of Cy7 (0.2 mg, 0.24  $\mu$ mol). After 2 h at room temperature the reaction mixture was purified by HPLC as in 800CW-1 to afford 0.2 mg (72%) of Cy7-2 (retention time = 17

min). ESI-Mass calcd for  $C_{53}H_{72}N_6O_{17}S_2$   $[M]^+$  1128.4, found 565.0  $[M+H]^{2+}$ , 1129.0  $[M]^+$ .

**Synthesis of Cy5.5-2.** To a solution of **2** (0.5 mg, 0.86  $\mu$ mol) in DMSO (0.1 mL) was added *N,N*-diisopropylethylamine (0.002 mL, 11.5  $\mu$ mol), followed by the NHS ester of Cy5.5 (0.2 mg, 0.18  $\mu$ mol). After 2 h at room temperature the reaction mixture was purified by HPLC as in 800CW-1 to afford 0.2 mg (83%) of Cy5.5-2 (retention time = 13 min). ESI-Mass calcd for  $C_{59}H_{74}N_6O_{23}S_4$   $[M]^+$  1362.4, found 681.9  $[M+H]^{2+}$ , 1362.7  $[M]^+$ .

**Synthesis of 800RS-3.** To a solution of **3**<sup>9</sup> (0.3 mg, 0.42  $\mu$ mol) in DMSO (0.1 mL) was added *N,N*-diisopropylethylamine (0.002 mL, 11.5  $\mu$ mol), followed by NHS ester of IRDye800RS (0.3 mg, 0.31  $\mu$ mol). After 2 h at room temperature the reaction mixture was purified by HPLC (column, Econosphere C18 5 $\mu$ , 150  $\times$  4.6 mm; retention time, 27 min; mobile phase, A = 0.1% TFA in H<sub>2</sub>O, B = 0.1% TFA in CH<sub>3</sub>CN; gradient, 0 mins = 0% B, 5 mins = 0% B, 45 mins = 100% B; flow rate, 1 mL/min) to afford 0.3 mg (67%) of 800RS-3 (retention time = 27 min). ESI-Mass calcd for  $C_{72}H_{97}N_7O_{19}S_2$   $[M]^+$  1427.6, found 714.4  $[M+H]^{2+}$ , 1427.8  $[M]^+$ .

**Synthesis of ICG-3.** To a solution of **3** (0.5 mg, 0.71  $\mu$ mol) in DMSO (0.1 mL) was added *N,N*-diisopropylethylamine (0.002 mL, 11.5  $\mu$ mol), followed by ICG-Sulfo-OSu (0.3 mg, 0.32  $\mu$ mol). After 2 h at room temperature the reaction mixture was purified by

HPLC as in 800RS-**3** to afford 0.3 mg (71%) of ICG-**3** (retention time = 32 min). ESI-Mass calcd for  $C_{71}H_{93}N_7O_{15}S$   $[M]^+$  1315.6, found 1316.0  $[M]^+$ .

**Synthesis of Cy7-3.** To a solution of **3** (0.5 mg, 0.71  $\mu$ mol) in DMSO (0.1 mL) was added *N,N*-diisopropylethylamine (0.002 mL, 11.5  $\mu$ mol), followed by the NHS ester of Cy7 (0.5 mg, 0.61  $\mu$ mol). After 2 h at room temperature the reaction mixture was purified by HPLC as in 800RS-**3** to afford 0.5 mg (64%) of Cy7-**3** (retention time = 19 min). ESI-Mass calcd for  $C_{61}H_{85}N_7O_{18}S_2$   $[M]^+$  1267.5, found 634.5  $[M+H]^{2+}$ , 1267.9  $[M]^+$ .

**Synthesis of Cy5.5-3.** To a solution of **3** (0.5 mg, 0.71  $\mu$ mol) in DMSO (0.1 mL) was added *N,N*-diisopropylethylamine (0.002 mL, 11.5  $\mu$ mol), followed by the NHS ester of Cy5.5 (0.5 mg, 0.44  $\mu$ mol). After 2 h at room temperature the reaction mixture was purified by HPLC as in 800RS-**3** to afford 0.6 mg (90%) of Cy5.5-**3** (retention time = 18 min). ESI-Mass calcd for  $C_{67}H_{87}N_7O_{24}S_4$   $[M]^+$  1501.5, found 751.4  $[M+H]^{2+}$ , 1501.6  $[M]^+$ .

## Biology

**In Vitro PSMA Inhibition Assay.** The PSMA binding affinities of the dye-urea conjugates for PSMA were measured using the NAALADase assay, as previously described.<sup>30,31</sup> PSMA is known also as glutamate carboxypeptidase II (GCPII), or NAALADase.<sup>32,33</sup> A reaction mixture (total volume of 50  $\mu$ L) containing [ $^3$ H]*N*-acetyl-aspartylglutamate ([ $^3$ H]NAAG, 30 nM, 1,850 GBq/mmol) and human recombinant

GCPII (40 pM final) in Tris-HCl (pH 7.4, 40 mM) containing 1 mM CoCl<sub>2</sub> was used. The reaction was carried out at 37°C for 15 min and stopped with ice-cold sodium phosphate buffer (pH 7.4, 0.1 M, 50 µL). Blanks were obtained by incubating the reaction mixture in the presence of 2-phosphonomethyl pentanedioic acid (2-PMPA, 1 µM final), a selective and potent inhibitor of PSMA.<sup>32</sup> Dye-urea conjugates and controls were tested at log-unit final concentrations, that ranged from 100 µM to < fM. A 90 µL aliquot from each terminated reaction was transferred to a well in a 96-well spin column containing AG1X8 ion- exchange resin. The plate was centrifuged at 1500 rpm for 5 min using a Beckman GS-6R centrifuge (Beckman Coulter, Inc., Brea, CA) equipped with a PTS-2000 rotor. [<sup>3</sup>H]NAAG bound to the resin and [<sup>3</sup>H]glutamate eluted in the flow-through. Columns were then washed twice with formate (1 M, 90 µL) to ensure complete elution of [<sup>3</sup>H]glutamate. The flow-through and the washes were collected in a deep 96-well block. From each well with a total volume of 270 µL, a 200 µL aliquot was transferred to its respective well in a solid scintillator-coated 96-well plate (Packard, Meriden, CT) and dried to completion. The radioactivity corresponding to [<sup>3</sup>H]glutamate was determined with a scintillation counter (Topcount NXT, Packard, counting efficiency 80%). IC<sub>50</sub> curves were generated from CPM results, by use of both Microsoft Office Excel 2007 and GraphPad Prism 5 programs, with *K<sub>i</sub>* values derived from the IC<sub>50</sub> values.<sup>34</sup>

**Cell Lines and Tumor Models.** PSMA+ PC3 PIP and PSMA non-expressing PC3 flu cell lines were originally a gift from Warren Heston (Cleveland Clinic Foundation<sup>35</sup>). Cells were cultured in RPMI 1640 medium (Mediatech, Manassas, VA) containing 10%

FBS (Sigma) and 1% penicillin-streptomycin (Mediatech) in a humidified incubator under 5% CO<sub>2</sub> at 37°C. Cells were cultured to 80% confluence and then trypsinized and collected. Two million cells each of PSMA+ PC3 PIP and PSMA- PC3 flu were re-suspended in 0.1ml PBS (Mediatech) and injected subcutaneously (s.c) into 4 – 6 week old male athymic nude mice (NCI, Frederick, MD) in the upper right and left flanks. Mice were used in imaging studies when tumors reached 3 – 5 mm in diameter.

***In Vivo Imaging and Ex Vivo Biodistribution.*** *In vivo* images with compounds Cy5.5-1, Cy5.5-2 and Cy5.5-3 were acquired on the IVIS Spectrum using an excitation wavelength of 675 nm and detection of the emission wavelength at 720 nm. The exposure time for each image acquisition was 1 sec. Images were scaled to the same maximum intensity using the supplier's software.

Compounds containing 800CW, 800RS, ICG derivative and Cy7 as fluorophores were imaged using the Pearl Impulse Imager. The Pearl imager is a dedicated fluorescence imaging instrument for mice and has fixed excitation wavelengths of 685 nm and 785 nm and emission wavelengths of 700 nm and 800 nm, respectively, as well as a white-light overlay. For *in vivo* studies, stock solutions (~ 1 mM) of dye-urea conjugates were prepared in H<sub>2</sub>O (compounds containing 800CW, 800RS, Cy5.5 and Cy7) or DMSO (compounds containing the ICG derivative) and were diluted with PBS for injection. After image acquisition at baseline (pre-injection), each mouse was injected intravenously with 1 nmol of dye-urea conjugate and images were acquired at 5 min, 1 h, 4 h and 24 h time points. Following the 24 h image each mouse was sacrificed by

cervical dislocation and tumor, muscle, liver, spleen, kidneys and intestine were collected and assembled on a petri dish for image acquisition. All images were scaled to the same maximum intensity for direct comparison. For quantification, regions of interest (ROI) were drawn over the organs displayed in *ex vivo* images ( $n = 4$ ) and fluorescence signal intensity of the organs was calculated using the supplier's software. Signal intensity of the muscle was set as background for all calculations. For binding specificity (blocking) studies, Cy7-**3** was co-injected with 1  $\mu\text{mol}$  of (*S*)-2-(3-((*S*)-1-carboxy-5-(4-iodobenzamido)pentyl)ureido)pentanedioic acid (DCIBzL, a known high-affinity PSMA inhibitor<sup>29</sup>) and images were acquired at 1, 4 and 24 h post-injection.

## RESULTS AND DISCUSSION

### Chemical Synthesis

Compound **1** is urea containing both lysine and glutamate substituents (a lysine-glutamate urea). It was obtained after deprotection of the *tert*-butyloxycarbonyl (Boc) and the *p*-methoxybenzyl (PMB) groups from compound **4**<sup>28</sup> as outlined in Scheme 1. Compound **2** has a short polyethylene glycol (PEG) linker. Compound **5**<sup>28</sup> was conjugated to Boc-NH(CH<sub>2</sub>CH<sub>2</sub>O)<sub>2</sub>CH<sub>2</sub>COOH to give compound **6**, which was then deprotected to provide compound **2**. Compound **3** has a lysine-suberate linker attached to the lysine-glutamate urea and it was prepared as previously reported.<sup>9</sup>

The commercially available amine-reactive active esters of IRDye800CW, IRDye800RS, the indocyanine green (ICG) derivative, Cy7 or Cy5.5 with principal excitation/emission wavelengths at 774/789, 767/786, 768/804, 743/767 and 675/694 nm,

respectively, were conjugated with **1**, **2** and **3** to produce the dye-PSMA inhibitors shown in Figure 1. Conjugation of activated esters of the NIR dyes to **1-3** were completed at room temperature within 2 h. The yields for these conjugates ranged from 53% to 90%.

### ***In Vitro* PSMA Inhibition**

The IC<sub>50</sub> values of the conjugates were measured using the *N*-acetylated- $\alpha$ -linked-acidic dipeptidase (NAALADase) assay<sup>30,31</sup> with results presented as  $K_i$  values in Table 1. The  $K_i$  values range from 1 – 700 pM, which is similar to other compounds of this class.<sup>9,28,29,36</sup> We observed a trend whereby agents with linkers, such as 800CW-**2**, ICG-**2**, Cy5.5-**2**, 800CW-**3**, ICG-**3**, and Cy5.5-**3** had lower  $K_i$  values than their counterparts with no linkers (800CW-**1**, ICG-**1**, and Cy5.5-**1**). However, Cy7 conjugates did not follow this trend and exhibited similar high affinities independent of the linker. This may be due to the smaller size of Cy7 compared to Cy5.5 and sulfo-ICG and the greater flexibility of the polyene moiety in Cy7 compared to the cyclohexene containing polyene in 800CW and 800RS dyes. Both effects could increase the accessibility of the urea to the PSMA binding site.

### **NIR Imaging and Biodistribution**

Among the five dyes tested in this study, only the Cy5.5-urea conjugates have excitation and emission wavelengths below 700 nm. Accordingly, imaging studies with Cy5.5-**1**, Cy5.5-**2**, and Cy5.5-**3** were undertaken on the Xenogen IVIS 200 system with excitation at 675 nm and emission at 720nm. Figure 2 shows images at 24 h after injection of 1 nmol of Cy5.5-**1**, Cy5.5-**2** and Cy5.5-**3** in mice with PSMA+ PC3 PIP and PSMA- PC3



flu tumors. All three compounds demonstrated high uptake within PSMA+ PC3 PIP tumors and little uptake in PSMA- PC3 flu tumors. The relative degree of observed PSMA+ PC3 PIP tumor uptake was in the order: Cy5.5-3 > Cy5.5-2 > Cy5.5-1. Renal uptake is due to high expression of PSMA within proximal renal tubules as well as to excretion, as previously shown.<sup>37-39</sup> Imaging of compounds containing 800CW, 800RS, the ICG derivative and Cy7 as fluorophores were conducted using the Pearl Imager, which has a set excitation wavelength at 785 nm and emission at 800 nm. These dye-urea conjugates have excitation and emission wavelengths above 700 nm, which allow for better depth of light penetration than compounds that emit at lower wavelengths and minimal autofluorescence. Figure 3 shows typical whole body and excised organ imaging of mice with PSMA+ PC3 PIP and PSMA- PC3 flu tumors at 24 h after injection of 1 nmol of the 800CW, 800RS, the ICG derivative or Cy7-urea conjugates. All compounds demonstrated PSMA+ PC3 PIP tumor uptake with little PSMA- PC3 flu tumor uptake, indicating target selectivity *in vivo*.

These images also demonstrate that the choice of dye and linking group have significant effects on biodistribution. Intense fluorescence signals were observed in both tumor and kidneys for all three IRDye800CW conjugates (800CW-1, 800CW-2 and 800CW-3) with 800CW-3 having much lower normal tissue uptake than the other two compounds. IRDye800RS has a similar structure, but with two less sulfonate groups compared to IRDye800CW. PSMA+ PIP tumor uptake was observed in all three 800RS-urea conjugates. However, the fluorescence intensities were significantly lower than for the corresponding 800CW conjugates. Among those three 800RS-urea conjugates, 800RS-3,

which has a lysine suberate linker, showed highest PSMA+ PIP tumor uptake. Similarly, among the three ICG-urea conjugates, ICG-**3**, gave the highest PSMA+ PIP tumor uptake. ICG-**3** also demonstrated higher PSMA+ PIP tumor uptake compared to kidney, which differs from 800CW-**3** and 800RS-**3**, which had roughly equivalent tumor and kidney uptake. Cy7-**2** and Cy7-**3** had significantly higher PSMA+ PIP tumor uptake than uptake in kidneys. They also demonstrated the lowest normal tissue uptake comparing to the other compounds with the same linker. From this preliminary evaluation we chose 800CW and Cy7 conjugates for further study, where the organs of 4 mice/agent were harvested and imaged at 24 h post-administration of imaging agent. Fluorescence intensity per organ is shown in Figure 4. In both the Cy7 series and the IRDye800CW series the degree of PSMA+ PIP tumor uptake was 800CW-**3** or Cy7-**3**  $\approx$  800CW-**2** or Cy7-**2** > 800CW-**1** or Cy7-**1**, confirming the importance of the linker moiety for modifying pharmacokinetics. Tumor to kidney ratios for Cy7-**2** and Cy7-**3** were higher than for 800CW-**2** and 800CW-**3**. The fluorescence intensities of all organs except the gastrointestinal tract for Cy7 conjugates were lower than for the corresponding 800CW conjugates. This is most likely because the Pearl Imager has a fixed excitation maximum at 785 nm and collects emission at 820 nm, which is further from the excitation and emission maxima of Cy7 (743/767) than those for IRDye800CW (774/789).

In order to demonstrate the PSMA-binding specificity of the PSMA inhibitor-dye conjugates, DCIBzL was co-administered with Cy7-**3**. As shown in Figure 5, all emission from the PSMA+ target tumor was blocked with concurrent DCIBzL

administration, indicating specific binding. The excised organ imaging results are consistent with the *in vivo* images.

The active site of PSMA possesses two binding sites, comprised of a pharmacophore (S1') site and an amphiphilic, non-pharmacophore (S1) site.<sup>40</sup> The S1' site is generated by amino acid residues highly sensitive to structural modification of potential ligands, demonstrating a strong preference for glutamate or glutamate-like residues. Compared to the S1' site, the S1 site is more promiscuous. A tunnel-like region (~ 20 Å) linked to the S1 site is projected toward the surface of the enzyme. Utilizing the tunnel region we have attached bulky chelated metals to the urea-based specificity-conferring moiety through a long linker to maintain the chelated metal entirely outside of protein. In so doing we have produced a small array of PSMA-targeted radiotracers capable of imaging PSMA in experimental models of prostate cancer.<sup>28,36,41</sup> Similarly, by attaching bulky fluorophores to the urea inhibitors through a linker, such as in dye-2 or dye-3 conjugates, the fluorophores can be situated outside of the active site, allowing maximum interaction with the urea-based specificity conferring portion of the agent. This effect is most noticeable in the higher tumor uptake demonstrated by 800RS-2, 800RS-3, ICG-2, ICG-3, and Cy5.5-3 compared to dye-1conjugates 800RS-1, ICG-1, and Cy5.5-1.

Recently Nakajima et al. have used the anti-PSMA antibody J591 conjugated to ICG to visualize PSMA+ tumors in whole mice at up to 10 days after administration.<sup>10</sup> We and others have focused on developing low molecular weight optical imaging agents for PSMA, in part to avoid the longer biological half-lives of antibody-based methods, to enable imaging at shorter times after administration.<sup>9,23,24,42-44</sup> However, to date most

such low molecular weight agents have only been used *in vitro*. Humblet et al. has reported *in vivo* imaging of PSMA-binding NIR-emitting phosphonate derivatives, however at 20 sec, the time of maximum PSMA-positive tumor uptake, the tumor to background ratio is less than two.<sup>24</sup> Previously we were able to image PSMA+ tissues in experimental models of prostate cancer using the targeted, IRDye800CW-based agent, YC-27 (800CW-3).<sup>9</sup> Here we used the same urea-based targeting moiety but expanded to the small series reported, investigating the pharmacokinetic effects of different linkers and fluorophores.

## CONCLUSION

Compounds **2** and **3**, which contain PEG and lysine-suberate linkers, respectively, provide useful scaffolds for optical imaging of PSMA. Although IRDye800CW and Cy7 conjugates 800CW-2, 800CW-3, Cy7-2, and Cy7-3 demonstrated high, PSMA-specific uptake *in vivo* at 24 h post-injection, the exact choice of dye for intra-operative imaging will depend upon the specifications of the camera used for detection in the operating suite. Nevertheless, this small series demonstrates that a variety of dyes with different absorption and emission spectra can be accommodated.

## ACKNOWLEDGMENTS

We thank CA134675 and the AdMeTech Foundation for financial support and Dr. Ron Rodriguez for helpful discussions.

## SUPPORTING INFORMATION

HPLC conditions and traces for the final compounds, ligated to the commercial and previously reported NIR dyes used herein, are provided: 800CW-1; 800CW-2; 800CW-3; 800RS-1; 800RS-2; 800RS-3; ICG-1; ICG-2; ICG-3; Cy7-1; Cy7-2; Cy7-3; Cy5.5-1; Cy5.5-2; Cy5.5-3. This material is available free of charge *via* the Internet at <http://pubs.acs.org>.

## ABBREVIATIONS

NIR: near-infrared

ICG: indocyanine green

PSMA: prostate-specific membrane antigen

NAAG: *N*-acetylaspartyl glutamate

NAALADase: *N*-acetylated- $\alpha$ -linked-acidic dipeptidase

Boc: *tert*-butoxycarbonyl

PMB: *p*-methoxybenzyl

PEG: polyethylene glycol

NHS: *N*-hydroxysuccinimide

DCIBzL: (*S*)-2-(3-(((*S*)-1-carboxy-5-(4-iodobenzamido)pentyl)ureido)pentanedioic acid

## REFERENCES

- (1) Siegel, R., Naishadham, D., and Jemal, A. (2012) Cancer statistics, 2012. *CA: a cancer journal for clinicians* 62, 10-29.
- (2) Bill-Axelsson, A., Holmberg, L., Ruutu, M., Garmo, H., Stark, J. R., Busch, C., Nordling, S., Haggman, M., Andersson, S. O., Bratell, S., Spangberg, A.,

Palmgren, J., Steineck, G., Adami, H. O., and Johansson, J. E. (2011) Radical prostatectomy versus watchful waiting in early prostate cancer. *N Engl J Med* 364, 1708-17.

(3) National Cancer Institute (2008) Surveillance Epidemiology and End Results (SEER). <http://seer.cancer.gov/data/>

(4) Hu, J. C., Wang, Q., Pashos, C. L., Lipsitz, S. R., and Keating, N. L. (2008) Utilization and outcomes of minimally invasive radical prostatectomy. *J Clin Oncol* 26, 2278-84.

(5) Gioux, S., Choi, H. S., and Frangioni, J. V. (2010) Image-guided surgery using invisible near-infrared light: fundamentals of clinical translation. *Mol Imaging* 9, 237-55.

(6) Frangioni, J. V. (2008) New technologies for human cancer imaging. *J Clin Oncol* 26, 4012-21.

(7) Ye, Y., Bloch, S., Xu, B., and Achilefu, S. (2006) Design, synthesis, and evaluation of near infrared fluorescent multimeric RGD peptides for targeting tumors. *Journal of medicinal chemistry* 49, 2268-75.

(8) Schaafsma, B. E., Mieog, J. S., Hutteman, M., van der Vorst, J. R., Kuppen, P. J., Lowik, C. W., Frangioni, J. V., van de Velde, C. J., and Vahrmeijer, A. L. (2011) The clinical use of indocyanine green as a near-infrared fluorescent contrast agent for image-guided oncologic surgery. *Journal of surgical oncology* 104, 323-32.

(9) Chen, Y., Dhara, S., Banerjee, S. R., Byun, Y., Pullambhatla, M., Mease, R. C., and Pomper, M. G. (2009) A low molecular weight PSMA-based fluorescent

1  
2  
3 imaging agent for cancer. *Biochemical and biophysical research communications* 390,  
4  
5 624-9.  
6

7  
8 (10) Nakajima, T., Mitsunaga, M., Bander, N. H., Heston, W. D., Choyke, P.  
9  
10 L., and Kobayashi, H. (2011) Targeted, activatable, in vivo fluorescence imaging of  
11  
12 prostate-specific membrane antigen (PSMA) positive tumors using the quenched  
13  
14 humanized J591 antibody-indocyanine green (ICG) conjugate. *Bioconjugate chemistry*  
15  
16 22, 1700-5.  
17  
18

19  
20 (11) Solomon, M., Liu, Y., Berezin, M. Y., and Achilefu, S. (2011) Optical  
21  
22 imaging in cancer research: basic principles, tumor detection, and therapeutic monitoring.  
23  
24 *Medical principles and practice : international journal of the Kuwait University, Health*  
25  
26 *Science Centre* 20, 397-415.  
27  
28

29  
30 (12) Silver, D. A., Pellicer, I., Fair, W. R., Heston, W. D., and Cordon-Cardo,  
31  
32 C. (1997) Prostate-specific membrane antigen expression in normal and malignant human  
33  
34 tissues. *Clin Cancer Res* 3, 81-5.  
35

36  
37 (13) Ghosh, A., and Heston, W. D. (2004) Tumor target prostate specific  
38  
39 membrane antigen (PSMA) and its regulation in prostate cancer. *J Cell Biochem* 91, 528-  
40  
41 39.  
42

43  
44 (14) Baccala, A., Sercia, L., Li, J., Heston, W., and Zhou, M. (2007)  
45  
46 Expression of prostate-specific membrane antigen in tumor-associated neovasculature of  
47  
48 renal neoplasms. *Urology* 70, 385-90.  
49

50  
51 (15) Chang, S. S., O'Keefe, D. S., Bacich, D. J., Reuter, V. E., Heston, W. D.,  
52  
53 and Gaudin, P. B. (1999) Prostate-specific membrane antigen is produced in tumor-  
54  
55 associated neovasculature. *Clin Cancer Res* 5, 2674-81.  
56  
57  
58  
59  
60

(16) Haffner, M. C., Kronberger, I. E., Ross, J. S., Sheehan, C. E., Zitt, M., Muhlmann, G., Ofner, D., Zelger, B., Ensinger, C., Yang, X. J., Geley, S., Margreiter, R., and Bander, N. H. (2009) Prostate-specific membrane antigen expression in the neovasculature of gastric and colorectal cancers. *Human pathology* 40, 1754-61.

(17) Milowsky, M. I., Nanus, D. M., Kostakoglu, L., Sheehan, C. E., Vallabhajosula, S., Goldsmith, S. J., Ross, J. S., and Bander, N. H. (2007) Vascular targeted therapy with anti-prostate-specific membrane antigen monoclonal antibody J591 in advanced solid tumors. *J Clin Oncol* 25, 540-7.

(18) Cho, S. Y., Gage, K. L., Mease, R. C., Senthamizhchelvan, S., Holt, D. P., Kwanisai-Jeffrey, A., Endres, C. J., Dannals, R. F., Sgouros, G., Lodge, M. A., Eisenberger, M. A., Rodriguez, R., Carducci, M. A., Rojas, C., Slusher, B. S., Kozikowski, A. P., and Pomper, M. G. (2012) Biodistribution, Tumor Detection and Radiation Dosimetry of N-[N-[(S)-1,3-Dicarboxypropyl]carbamoyl]-4-18F-fluorobenzyl-L-cysteine (18F-DCFBC), a Low Molecular Weight Inhibitor of PSMA, in Patients with Metastatic Prostate Cancer. *J Nucl Med* in press.

(19) Barrett, J. S., LaFrance, N., Coleman, R. E., Goldsmith, S. J., Stubbs, J. B., Petry, N. A., Vallabhajosula, S., Maresca, K. P., Femia, F. J., and Babich, J. W. In *Annual Meeting of the Society of Nuclear Medicine* 2009, p 136P.

(20) Babich, J., Coleman, R. E., Van Heertum, R., Vallabhajosula, S., Goldsmith, S., Osborne, J., Slawin, K., and Joyal, J. In *Annual Meeting of the Society of Nuclear Medicine* 2012, p 179P.

(21) Afshar-Oromieh, A., Haberkorn, U., Eder, M., Eisenhut, M., and Zechmann, C. M. (2012) [68Ga]Gallium-labelled PSMA ligand as superior PET tracer



for the diagnosis of prostate cancer: comparison with  $^{18}\text{F}$ -FECH. *Eur J Nucl Med Mol Imaging* 39, 1085-6.

(22) Kularatne, S. A., Wang, K., Santhapuram, H. K., and Low, P. S. (2009) Prostate-specific membrane antigen targeted imaging and therapy of prostate cancer using a PSMA inhibitor as a homing ligand. *Mol Pharm* 6, 780-9.

(23) Liu, T., Wu, L. Y., Hopkins, M. R., Choi, J. K., and Berkman, C. E. (2010) A targeted low molecular weight near-infrared fluorescent probe for prostate cancer. *Bioorg Med Chem Lett* 20, 7124-6.

(24) Humblet, V., Lapidus, R., Williams, L. R., Tsukamoto, T., Rojas, C., Majer, P., Hin, B., Ohnishi, S., De Grand, A. M., Zaheer, A., Renze, J. T., Nakayama, A., Slusher, B. S., and Frangioni, J. V. (2005) High-affinity near-infrared fluorescent small-molecule contrast agents for in vivo imaging of prostate-specific membrane antigen. *Mol Imaging* 4, 448-62.

(25) Elsasser-Beile, U., Reischl, G., Wiehr, S., Buhler, P., Wolf, P., Alt, K., Shively, J., Judenhofer, M. S., Machulla, H. J., and Pichler, B. J. (2009) PET imaging of prostate cancer xenografts with a highly specific antibody against the prostate-specific membrane antigen. *J Nucl Med* 50, 606-11.

(26) Bander, N. H., Trabulsi, E. J., Kostakoglu, L., Yao, D., Vallabhajosula, S., Smith-Jones, P., Joyce, M. A., Milowsky, M., Nanus, D. M., and Goldsmith, S. J. (2003) Targeting metastatic prostate cancer with radiolabeled monoclonal antibody J591 to the extracellular domain of prostate specific membrane antigen. *J Urol* 170, 1717-21.

(27) Yao, D., Trabulsi, E. J., Kostakoglu, L., Vallabhajosula, S., Joyce, M. A., Nanus, D. M., Milowsky, M., Liu, H., and Goldsmith, S. J. (2002) The utility of monoclonal antibodies in the imaging of prostate cancer. *Semin Urol Oncol* 20, 211-8.

(28) Banerjee, S. R., Foss, C. A., Castanares, M., Mease, R. C., Byun, Y., Fox, J. J.; Hilton, J., Lupold, S. E., Kozikowski, A. P., and Pomper, M. G. (2008) Synthesis and evaluation of technetium-99m- and rhenium-labeled inhibitors of the prostate-specific membrane antigen (PSMA). *Journal of medicinal chemistry* 51, 4504-17.

(29) Chen, Y., Foss, C. A., Byun, Y., Nimmagadda, S., Pullambahatla, M., Fox, J. J., Castanares, M., Lupold, S. E., Babich, J. W., Mease, and R. C., Pomper, M. G. (2008) Radiohalogenated Prostate-Specific Membrane Antigen (PSMA)-Based Ureas as Imaging Agents for Prostate Cancer. *Journal of medicinal chemistry* 51, 7933-7943.

(30) Robinson, M. B., Blakely, R. D., Couto, R., and Coyle, J. T. (1987) Hydrolysis of the brain dipeptide N-acetyl-L-aspartyl-L-glutamate. Identification and characterization of a novel N-acetylated alpha-linked acidic dipeptidase activity from rat brain. *J Biol Chem* 262, 14498-506.

(31) Rojas, C., Frazier, S. T., Flanary, J., and Slusher, B. S. (2002) Kinetics and inhibition of glutamate carboxypeptidase II using a microplate assay. *Anal Biochem* 310, 50-4.

(32) Jackson, P. F., Cole, D. C., Slusher, B. S., Stetz, S. L., Ross, L. E., Donzanti, B. A., and Trainor, D. A. (1996) Design, synthesis, and biological activity of a potent inhibitor of the neuropeptidase N-acetylated alpha-linked acidic dipeptidase. *Journal of medicinal chemistry* 39, 619-22.

- (33) Foss, C. A., Mease, R. C., Cho, S. Y., Kim, H. J., and Pomper, M. G. (2012) GCPII imaging and cancer. *Curr Med Chem* 19, 1346-59.
- (34) Cheng, Y., and Prusoff, W. H. (1973) Relationship between the inhibition constant ( $K_i$ ) and the concentration of inhibitor which causes 50 percent inhibition ( $I_{50}$ ) of an enzymatic reaction. *Biochem Pharmacol* 22, 3099-3108.
- (35) Ghosh, A., Wang, X., Klein, E., and Heston, W. D. (2005) Novel role of prostate-specific membrane antigen in suppressing prostate cancer invasiveness. *Cancer*
- (36) Banerjee, S. R., Pullambhatla, M., Byun, Y., Nimmagadda, S., Foss, C. A., Green, G., Fox, J. J., Lupold, S. E., Mease, R. C., and Pomper, M. G. (2011) Sequential SPECT and optical imaging of experimental models of prostate cancer with a dual modality inhibitor of the prostate-specific membrane antigen. *Angewandte Chemie (International ed)* 50, 9167-70.
- (37) Silver, D. A., Pellicer, I., Fair, W. R., Heston, W. D., and Cordon-Cardo, C. (1997) Prostate-specific membrane antigen expression in normal and malignant human tissues. *Clinical cancer research : an official journal of the American Association for Cancer Research* 3, 81-5.
- (38) de la Taille, A., Cao, Y., Sawczuk, I. S., Nozemu, T., d'Agati, V., McKiernan, J. M., Bagiella, E., Buttyan, R., Burchardt, M., Olsson, C. A., Bander, N., and Katz, A. E. (2000) Detection of prostate-specific membrane antigen expressing cells in blood obtained from renal cancer patients: a potential biomarker of vascular invasion. *Cancer Detect Prev* 24, 579-88.

- (39) Kinoshita, Y., Kuratsukuri, K., Landas, S., Imaida, K., Rovito, P. M., Jr., Wang, C. Y., and Haas, G. P. (2006) Expression of prostate-specific membrane antigen in normal and malignant human tissues. *World J Surg* 30, 628-36.
- (40) Mesters, J. R., Barinka, C.; Li, W., Tsukamoto, T., Majer, P., Slusher, B. S., Konvalinka, J., and Hilgenfeld, R. (2006) Structure of glutamate carboxypeptidase II, a drug target in neuronal damage and prostate cancer. *Embo J* 25, 1375-84.
- (41) Banerjee, S. R., Pullambhatla, M., Byun, Y., Nimmagadda, S., Green, G., Fox, J. J., Horti, A., Mease, R. C., and Pomper, M. G. (2010) 68Ga-labeled inhibitors of prostate-specific membrane antigen (PSMA) for imaging prostate cancer. *Journal of medicinal chemistry* 53, 5333-41.
- (42) Liu, T., Wu, L. Y., Kazak, M., and Berkman, C. E. (2008) Cell-Surface labeling and internalization by a fluorescent inhibitor of prostate-specific membrane antigen. *Prostate* 68, 955-64.
- (43) Kularatne, S. A., Venkatesh, C., Santhapuram, H. K., Wang, K., Vaitilingam, B., Henne, W. A., and Low, P. S. (2010) Synthesis and biological analysis of prostate-specific membrane antigen-targeted anticancer prodrugs. *Journal of medicinal chemistry* 53, 7767-77.
- (44) Humblet, V., Misra, P., Bhushan, K. R., Nasr, K., Ko, Y. S., Tsukamoto, T., Pannier, N., Frangioni, J. V., and Maison, W. (2009) Multivalent scaffolds for affinity maturation of small molecule cell surface binders and their application to prostate tumor targeting. *Journal of medicinal chemistry* 52, 544-50.

# FIGURES

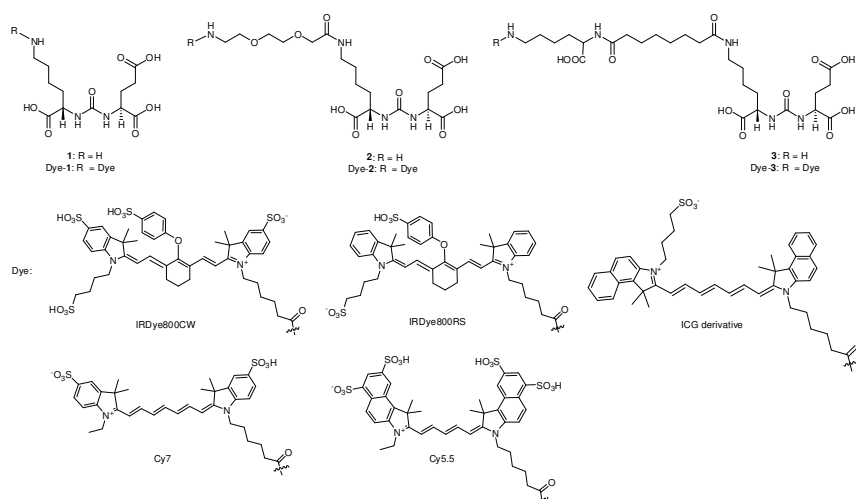


**Figure 1.** Structures of PSMA-based near-infrared fluorescent imaging agents.

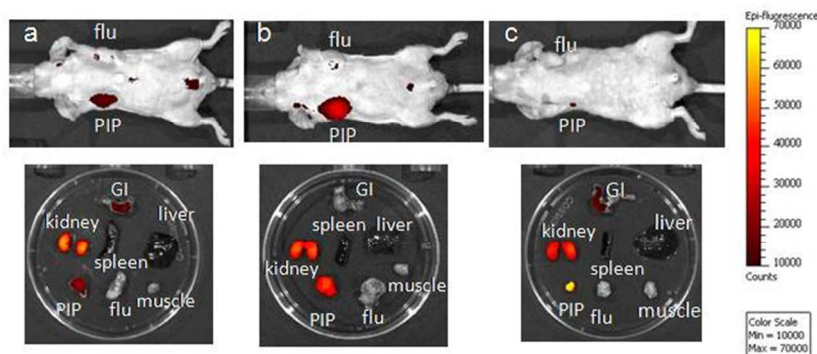


**Figure 2.** Whole body and *ex vivo* organ imaging of mice with PSMA+ PC3 PIP and PSMA- PC3 flu tumors at 24 h post-injection of 1 nmol of (a) Cy5.5-1, (b) Cy5.5-2 and (c) Cy5.5-3.

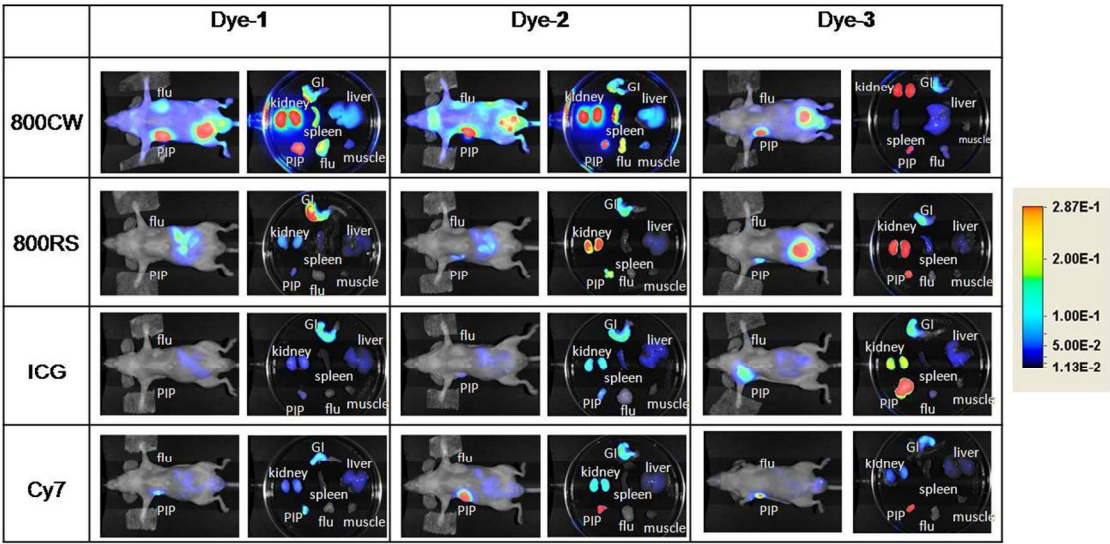


**Figure 3.** Whole body and *ex vivo* organ imaging of mice with PSMA+ PC3 PIP and PSMA- PC3 flu tumors at 24 h post-injection of 1 nmol of the indicated dye-urea conjugates.

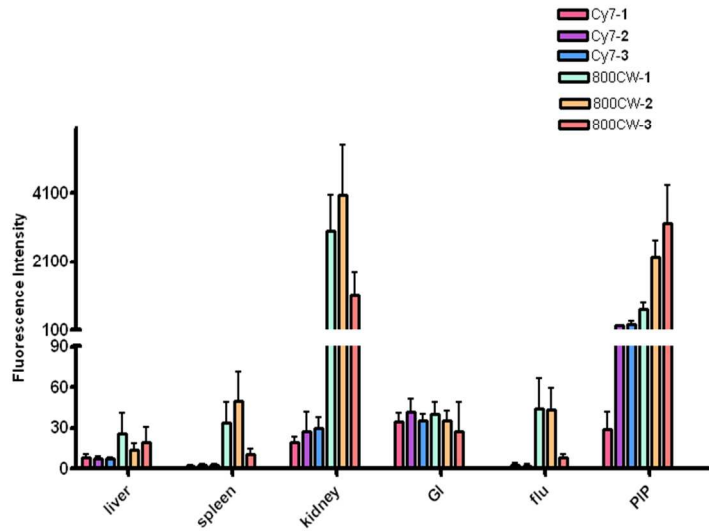


**Figure 4.** Biodistribution data at 24 h post-injection from regions of interest (ROI) drawn over organs displayed in *ex vivo* images and normalized to muscle. Four animals were imaged per agent. Values are represented as mean  $\pm$  SEM.

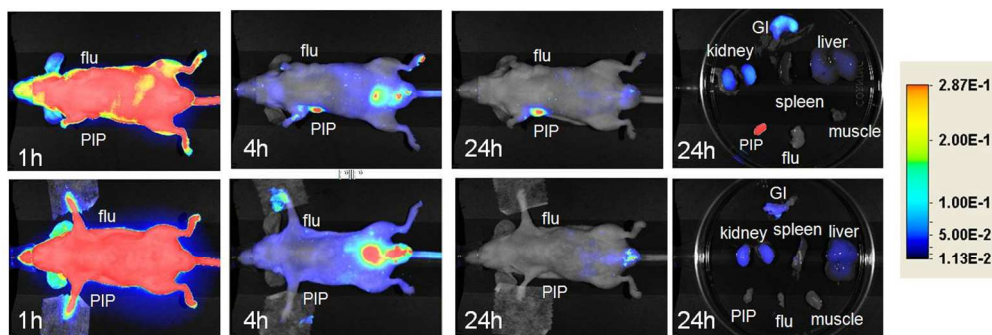
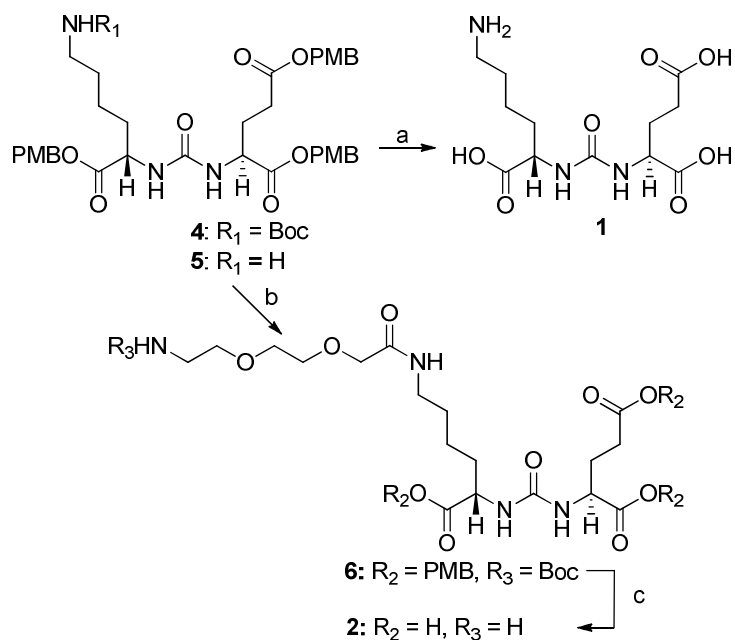


**Figure 5.** Top row: Images after administration of 1 nmol Cy7-3 at (left to right) 1 h, 4 h and 24 h post-injection, as well as images of the excised organs at 24 h post-injection.

Bottom row: Image after administration of 1 nmol Cy7-3 + 1 mmol DCIBzL, a high-affinity ligand for PSMA (blocker) at same time points as above. Note lack of uptake in the mice treated with DCIBzL, indicating binding specificity.





**Scheme 1.** a) TFA/anisole; b) Boc-NH(CH<sub>2</sub>CH<sub>2</sub>O)<sub>2</sub>CH<sub>2</sub>COOH, TBTU, *N,N*-diisopropylethylamine; c) TFA/anisole.

**Table 1.** PSMA *in Vitro* Inhibitory Activities

Compound	<i>K<sub>i</sub></i> (pM)
800CW-1	70±5 <sup>a</sup>
800CW-2	40±10 <sup>a</sup>
800CW-3	20±5 <sup>a</sup>
800RS-1	100±10 <sup>*b</sup>
800RS-2	200±50 <sup>a</sup>
800RS-3	4±0.5 <sup>b</sup>
ICG-1	700±10 <sup>*b</sup>
ICG-2	400±60 <sup>*b</sup>
ICG-3	200±5 <sup>*b</sup>
Cy7-1	1±0.5 <sup>b</sup>
Cy7-2	7±0.4 <sup>a</sup>
Cy7-3	5±0.2 <sup>b</sup>
Cy5.5-1	90±40 <sup>a</sup>
Cy5.5-2	50±20 <sup>a</sup>
Cy5.5-3	50±2 <sup>b</sup>

Values are in *K<sub>i</sub>* ± SEM  
<sup>a</sup> n=4, <sup>b</sup> n = 2, \*Measured in DMSO; all others in water

Figure 1 consists of two panels. The left panel shows a mouse at 24h post-injection with bioluminescence in the liver (flu) and PIP. The right panel shows ex vivo organs at 24h post-injection with bioluminescence in the liver, kidney, spleen, and muscle, with PIP and flu also labeled.

